Journal of Reliability
Science and
Engineering

PAPER • OPEN ACCESS

D-optimality criterion-based optimization design for cyclic combined stress accelerated degradation test

To cite this article: Xuefeng Kong *et al* 2026 *J. Reliab. Sci. Eng.* **2** 025201

View the article online for updates and enhancements.

You may also like

- A review of modelling and data analysis methods for accelerated test
Yashun Wang, Xun Chen, Shufeng Zhang et al.
- Optimal Design of Multi-Stress Accelerated Degradation Test within Irregular Test Region
Jinyan Guo, Zhaojun Yang, Chuanhai Chen et al.
- Structured Method to Reconfigure the Fatigue of Mechanical Products such as HKS in a Refrigerator
Seong-woo Woo, Dennis L. O'Neal, Yimer Mohammed Hassen et al.

This content was downloaded from IP address 118.123.172.210 on 26/05/2026 at 06:45

OPEN ACCESS
IOP Publishing | ISECAEP
Journal of Reliability Science and Engineering
J. Reliab. Sci. Eng. **2** (2026) 025201 (13pp)
https://doi.org/10.1088/3050-2454/ae64c7

D-optimality criterion-based optimization design for cyclic combined stress accelerated degradation test

Xuefeng Kong, Yinjing Wang, Jun Pan* and Wenhua Chen

Zhejiang Key Laboratory of Reliability Technology for Mechanical & Electrical Product, Zhejiang Sci-Tech University, Hangzhou 310018, People's Republic of China

E-mail: panjun@zstu.edu.cn

Received 4 January 2026, revised 28 March 2026
Accepted for publication 24 April 2026
Published 14 May 2026

Abstract

The multi-stress accelerated degradation test (ADT) scheme has recently garnered extensive attention owing to its effective acceleration parameters and strong alignment with engineering practice. Under this scheme, engineering products in practice typically need to traverse multiple task profiles, whereby they are subjected to alternating effects of multi-stresses. However, most studies overlook this feature and instead assume that multiple stresses are applied simultaneously, resulting in the associated test schemes failing to truly reflect the actual product degradation performance. To address this limitation, this study targets optimizing the cyclic combined stress ADT (CCSADT) scheme design. Specifically, a CCS ADM based on cumulative damage theory is initially proposed, applying which the product degradation process under the alternating action of multi-stresses can be captured effectively. Subsequently, the optimization objective of the CCSADT, considering minimization of the variance in model parameter estimation, is constructed on the basis of the D-optimality criterion. An optimization design model with the constraints of test time and test cost is then developed to obtain the optimal configuration for the number of cycles, stress level, and time for each cycle. Finally, the superiority of the proposed method over prior approaches is illustrated using a numerical example of an electrical connector.

Keywords: accelerated degradation test, cyclic combined stress, cumulative damage theory, D-optimality criterion

1. Introduction

With the continuous advancement of modern industrial products to achieve high reliability and long lifespans, conventional life tests have become less effective in meeting the rapid reliability assessment demands for products owing to the significant time and costs involved. Therefore, to address this predicament and derive product lifetimes within shorter periods of time, accelerated tests have been widely applied, as part of which the failure process is accelerated by increasing the stress levels that a product is exposed to [1]. However, for complex and particularly safety-critical products, collecting failure time data is often impractical owing to economic and safety considerations. This challenge has prompted researchers to utilize product degradation signals to reflect the health status of products, resulting in the development of the accelerated degradation test (ADT).

* Author to whom any correspondence should be addressed.

Original content from this work may be used under the terms of the Creative Commons Attribution 4.0 licence. Any further distribution of this work must maintain attribution to the author(s) and the title of the work, journal citation and DOI.

© 2026 The Author(s). Published by IOP Publishing Ltd on behalf of the Institute of Systems Engineering, China Academy of Engineering Physics

ADTs primarily comprise the AD model (ADM) and the test optimization criterion. The ADM, in turn, contains the accelerated and degradation models, and the construction of the accelerated model serves as the core link connecting the stress conditions with the product life characteristic. Commonly employed single-stress accelerated models include the Arrhenius model and inverse power-law model, whereas commonly employed degradation models include stochastic process models such as the Wiener process model [2], gamma process model [3], and inverse Gaussian process model [4], as well as general trajectory models such as the mixed effect model [5]. In this context, Zheng *et al* [6] considered the heterogeneity of the units and used nonlinear acceleration models and inverse Gaussian processes to depict the accelerated aging data. Similarly, Kang *et al* [7] estimated the remaining useful life of bipolar junction transistors by applying the Arrhenius model and gamma process and also processing the test data obtained from the ADT conducted at different temperatures. Chio *et al* [8] fitted a biexponential model based on the Arrhenius model to the degradation data and combined it with a mixed-effects modeling method to predict the long-term durability of proton exchange membrane fuel cell stacks under normal operating conditions. In another study, Li *et al* [9] developed a random effect model by combining the linear model with the Wiener process and verified the superiority of this model through the case study of cables. However, despite their advantages, all the aforementioned models require a clear, formal assumption. By contrast, the proportional hazards model (PHM) does not require the life or degradation quantity to follow a specific distribution; instead, it assumes that the stress variable affects the risk function in an exponential form. Such a semi-parametric structure enhances the robustness of the model. In a related study, Hu and Chen [10] proposed a Weibull PHM that jointly incorporates degradation data and lifetime data and derived a closed-form expression for the remaining useful life distribution to support the optimization of predictive maintenance strategies. Gao *et al* [11] also employed the PHM to jointly incorporate degradation data and failure time data and proposed an adaptive method for remaining useful life prediction.

With the diversification of modern product operating environments, a single stress is often insufficient to describe real degradation mechanisms, and research on ADMs has extended from single-stress models to multi-stress models. Commonly applied multi-stress accelerated models mainly include the Peck model and generalized Eyring model. In this regard, Huang *et al* [12] proposed a degradation testing model based on the Wiener process under multiple stresses by linking the drift coefficient to the stress factor through a logarithmic linear relationship. Similarly, Jiang *et al* [13] utilized the Wiener process to fit the degradation trajectory of electrical connector performance and combined it with the generalized Eyring model to evaluate the average lifespan of electrical connectors. Li *et al* [14] linked the generalized Eying model with the drift coefficient of the Wiener process and estimated the unknown parameters in the model using the maximum likelihood estimation-simulated annealing optimization search algorithm. Likewise, Liu *et al* [15] established a random-effect Wiener degradation model, considering temperature and humidity as the accelerating stresses and residual working current as the degradation characteristic, and combined it with the Peck model to calculate service life. Additionally, considerable research advancements have also been achieved in the PHM-based multi-stress ADT. For example, Zheng *et al* [16] proposed a novel PHM framework that incorporates both degradation trends and environmental factors as covariates and derived a closed-form reliability expression using a first-order Taylor approximation. Moreover, Monsour *et al* [17] studied two semi-parametric models, namely, the modified proportional hazard rate model and modified proportional reversed hazard rate model; by assuming that the external parameters of the candidate models were generally different, they determined several relative ranking attributes of both the investigated models.

Besides, the optimal design of ADT highly depends on the test optimization criterion. Commonly used test design optimality criterions include A-optimality, D-optimality, and V-optimality. Among these, the D-optimality criterion seeks to minimize the generalized variance of parameter estimates by maximizing the determinant of the Fisher information matrix, thereby achieving the highest overall information efficiency and the greatest precision in joint parameter estimation among the three criteria. Consequently, it has been widely adopted in the optimal design of various ADTs. For instance, Yan *et al* [18] modeled degradation using the Tweedie exponential dispersion process and proposed a step-stress ADT scheme optimized under the D-optimality criterion. Subsequently, they developed an optimal constant-stress ADT plan based on the same criterion, with stress levels constrained between prescribed minimum and maximum values [19]. Zhi [20] focused on the Wiener process with random initial value and conducted optimization design on ADTs under both single stress and multiple stress conditions based on the D-optimality criterion. Based on the Wiener degradation process as well, Li *et al* [21] proposed a constant stress accelerated degradation model incorporating multiple stress couplings and employed the D-optimality criterion to minimize the variance of parameter estimates. Jin *et al* [22] considered multiple performance degradation characteristics, modeled them using the Wiener process and Copula function, and proposed a multivariate ADT optimization method based on the D-optimality criterion.

Notably, the aforementioned studies primarily consider the simultaneous effects of multiple stresses on the product. However, for products that need to perform multi-stage tasks, the working condition stresses change with variations in the tasks. In the case of electrical connectors, which are critical components required for realizing the electrical connection of weapons and equipment, the key failure mode is contact failure due to excessive contact resistance. In practice, these weapons and equipment repeatedly switch between inventory and combat-readiness-duty statuses as required, during which electrical connectors repeatedly traverse the task profiles of storage, transportation, and testing. When the electrical connector is subjected to the storage profile, its metal surface

undergoes an oxidation reaction to form an interfacial film, leading to an increase in contact resistance; in this case, the main sensitive stress is temperature. When subjected to the transportation profile, the connector experiences fretting wear between its contact components. This wear degrades the protective coating and exposes the underlying copper substrate to air. Copper rapidly forms a native oxide film upon exposure, leading to an instantaneous increase in contact resistance when the contact points engage within this oxidized region [23]. Simultaneously, fretting wear can remove pre-existing oxide films formed during prior storage and testing profiles, thereby re-exposing the base material to air and initiating new oxidation reactions under subsequent storage or testing profiles [24]. Consequently, both the interfacial oxide film thickness and the contact resistance increase, and the primary sensitive stress within this profile is attributed to vibration. Finally, when the connector is subjected to the testing profile, the application of electrical stress causes the temperature of the contact piece to rise owing to the existence of contact resistance, thereby accelerating the rates of both surface oxidation and increase in contact resistance; in this case, the primary sensitive stress within this profile is attributed to electrical stress. Therefore, in this manner, the multitask profile exposes electrical connectors to different sensitive stresses under various task phases, and the alternating cycles of these multiple stresses further accelerate the degradation rate. Consequently, to truly reflect the product degradation process under different sensitive stresses and at different task stages, arriving at combined stress (CS) ADT optimization designs is required.

To the best of our knowledge, optimization design for CSADTs has only been explored by Li [25] and Xia [26]. Li experimentally implemented a specific type of active frequency-selective surface absorber under the CSs of temperature and vibration through a stepwise stress-ADT and constructed an artificial neural network-based Wiener process for reliability evaluation. By contrast, Xia developed a CS testing scheme for electrical connectors that considers the effects of vibration and temperature as well as insertion and extraction stresses to assess the storage reliability of these connectors. However, these researchers have only focused on the aging laws under simple sequential stress. In these tests, upon determining the types of sensitive stresses under each profile, the entire procedure is carried out by sequentially performing a single ADT at each type of stress condition with a certain stress level and duration time. Consequently, the alternating cyclic effect of multiple stresses is neglected, which results in a significant deviation between the product degradation process under the designed test scheme and the actual failure process.

To address this gap, this study investigates an optimization design for the cyclic CSADT (CCSADT) by considering the differences in sensitive stress at different task stages and the alternating cyclic effect of multiple stresses on the degradation process. The flowchart of the proposed method is illustrated in figure 1. First, to capture product degradation performance under the CCSADT, a generalized ADM is established based on the PHM. Subsequently, leveraging the cumulative damage theory, a general expression for the reliability function under the CCS profile is derived. Finally, an optimization objective of maximizing the accuracy of parameter estimation is formulated using the D-optimality criterion, and a CCSADT optimization design model is then constructed to obtain the optimal CS levels and test time under each cycle. The key contributions of the study are summarized below.

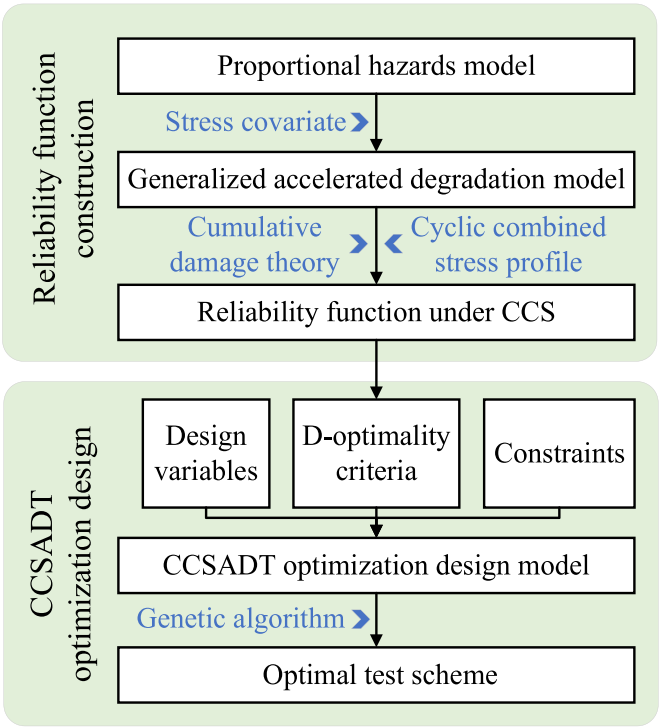


Figure 1. The flowchart of the proposed method.

(1) On the basis of the cumulative damage theorem, a generalized ADM combined with the PHM is constructed, which characterizes the profile-dependent differences in sensitive stress and alternating cyclic effect of multiple stresses, to accurately evaluate product reliability at any cycle and under any profile.
(2) For the first time, an optimization design model for the CCSADT is proposed on the basis of the D-optimality criterion, applying which the optimal CS levels and test time under each cycle are determined to acquire experimental data that better align with practical product degradation processes.

The remainder of this paper is organized as follows. Section 2 introduces the CCS profile and construction of a PHM-based reliability model. In section 3, the development of the optimization objective on the basis of the D-optimality criterion is described, along with an account of the optimization design model to obtain the CCSADT scheme. Section 4 provides details on the model implementation and effectiveness through a numerical study. Finally, section 5 provides concluding remarks and possible directions for future research.

2. CCS description and reliability model construction

In this section, the CCS profile description and failure definition of the product are first provided; subsequently, the procedure for establishing the reliability model of the product is described for the defined CCS profile, according to the PHM and cumulative damage theory.

2.1. CCS profile description

As described in section 1, the product in practical engineering is employed to experience a CCS profile, the process for which is expressed in figure 2. Specifically, in the CCS profile, each cycle consists of several profiles, and the product traverses these profiles in sequence. A detailed description of the CSS profile and failure definition of the products follows.

(1) Each profile is associated with a primary sensitive stress.
(2) There exist m cycles in the full life cycle of the products, and each cycle consists of n profiles. The stress level in the ith cycle and under the j th profile is denoted as $z_{i,j}$, where $i = 1,2,\cdots,m, j = 1,2,\cdots,n$.
(3) The time proportion of each profile within a single cycle is constant, and the proportional value of the ith profile can be denoted as r_j. Additionally, the test time of the ith cycle is denoted as τ_i.
(4) Different types of stresses affect the degradation performance of the products primarily in two ways: the first is on the degradation rate (e.g. the high temperature and humidity accelerate the product degradation process [27]), and the second is on the degradation level (e.g. as mentioned in the introduction, the vibration causes an instantaneous increase in contact resistance). Particularly, if the stress has the second kind of effect under the qth $(1 < q \leq n)$ profile, the instantaneous damage is proportional to the stress level with a correlation coefficient K.
(5) N samples are employed for testing, and the degradation level of the samples is tested simultaneously at the end of each profile. Therefore, the degradation level of the cth sample at the end of the jth profile in the ith cycle is denoted as $X_{i,j,c}$.
(6) Let x_0 denote the initial degradation level of the product for the case wherein the degradation path monotonically decreases, and failure occurs when the degradation level drops below the failure threshold D. Additionally, the failure mechanism of the product during the test remains unchanged.

2.2. Construction of ADM based on PHM

Given that the PHM does not require the prior assumption of a degradation path, it possesses wide applicability. Therefore, the PHM is adopted here to construct the ADM, which is expressed as:

$$h(x_t;t,z) = h_0(x_t;t)\exp(\beta z) \tag{1}$$

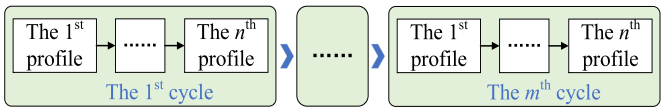


Figure 2. Schematic of CCS profile.

where $h(x_t;t,z)$ represents the failure rate at a degradation level of x_t, time t, and under stress z; $h_0(x_t;t)$ represents the basic failure rate at time t, and β is the influence coefficient of stress z.

According to Cai *et al* [28], the baseline degradation risk function can be divided into two separable functions of time and degradation, i.e.:

$$h_0(x_t;t) = p_0(x_t)\,u_0(t) \tag{2}$$

where $p_0(x_t)$ is a positive function of the degradation level x_t, and $u_0(t)$ is a function of time t. According to Eghbali and Elsayed [29], when the degradation path decreases monotonically, $p_0(x_t)$ should satisfy:

$$\int_0^{\infty} p_0(y)\,\mathrm{d}y = \infty \tag{3}$$

and $u_0(t)$ should satisfy:

$$\lim_{t\to 0} u_0(t) = 0. \tag{4}$$

Therefore, the expression presented by Wang and Coit [30] is used to model these two functions, which can be written as:

$$p_0(x_t) = a x_t^{a-1}, u_0(t) = t. \tag{5}$$

Consequently, equation (1) can be rewritten as:

$$h(x_t;t,z) = a x_t^{a-1} t \exp(\beta z). \tag{6}$$

2.3. Reliability function construction under CCS

If the degradation level of the product measured at time t is $x_t = l$, let T_D represent the time required for the product to degrade from the initial degradation level x_0 to D. Therefore, the reliability of the product at time t, given the condition of $x_t = l$, can be calculated as

$$R(t|x_t = l) = P(T_D > t|x_t = l). \tag{7}$$

Notably, $P(T_D > t|x_t = l) = 0$ when $l < D$, as the product fails once the degradation level is less than D, and $P(T_D > t|x_t = l) = 1$ when $l > D$. Subsequently, let $f(x_t;t,z)$ represent the probability density function of the degradation level at time t under stress z. According to the failure rate provided in equation (6), we can deduce that:

$$f(l;t,z) = \exp\left[-\int_{x_t}^{x_0} h(l;t,z)\,\mathrm{d}l\right]. \tag{8}$$

Consequently, the reliability function of the product at time t can be obtained on the basis of the total probability formula as

$$\begin{aligned} R(t) &= \int_0^{x_0} P(T_D > t | x_t = l) f(l;t,z)\,\mathrm{d}l \\ &= \int_0^{D} P(T_D > t | x_t = l) f(l;t,z)\,\mathrm{d}l \\ &\quad + \int_D^{x_0} P(T_D > t | x_t = l) f(l;t,z)\,\mathrm{d}l \\ &= \int_D^{x_0} f(l;t,z)\,\mathrm{d}l = P(l > D) \\ &= \exp\left[-\int_D^{x_0} h(l;t,z)\,\mathrm{d}l\right]. \end{aligned} \tag{9}$$

In particular, the reliability during the first profile at the first cycle can be obtained according to equation (9) as

$$\begin{aligned} R_{1,1}(t) &= \exp\left[-\int_D^{x_0} a l^{a-1} t \exp(\beta_1 z_{1,1})\,\mathrm{d}l\right] \\ &= \exp\left[-(x_0^a - D^a)\, t \exp(\beta_1 z_{1,1})\right]. \end{aligned} \tag{10}$$

During the qth profile in the first cycle, i.e., when the stress simultaneously affects the degradation rate and degradation level, the reliability can be expressed as

$$\begin{aligned} R_{1,q}(t - t_{q-1} + s_{q-1}) &= \int_{D+Kz_q}^{x_0} [p_0(l)\, q_0(t - t_{q-1} + s_{q-1}) \\ &\quad \cdot \exp(\beta_q z_{1,q})]\,\mathrm{d}l \\ &= \exp\left[-\left(x_0^a - (D + Kz_{1,q})^a\right)\right. \\ &\quad \left. \cdot (t - t_{q-1} + s_{q-1}) \exp(\beta_q z_{1,q})\right] \end{aligned} \tag{11}$$

where s_{q-1} represents the equivalent starting time under stress level $z_{1,q}$ at the first cycle, which is the equivalent time for converting the damage undergone in previous stages to the current stress level. According to the cumulative damage theory [31], the reliability of the product at the end of the $(q-1)$ th profile should be equal to that at the beginning of the qth profile, i.e.:

$$R_{1,(q-1)}(t_{q-1} - t_{q-2} + s_{q-2}, z_{1,q-1}) = R_{1,q}(s_{q-1}, z_{1,q}). \tag{12}$$

Hence, on the basis of equations (10) and (11), the detailed expression of s_{q-1} can be obtained as

$$s_{q-1} = \frac{(t_{q-1} - t_{q-2} + s_{q-2}) \exp(\beta_{q-1} z_{1,q-1})}{\exp(\beta_q z_{1,q})}. \tag{13}$$

Moreover, for the second cycle, the reliability during the first profile can be expressed as:

$$\begin{aligned} R_{2,1}(t - t_n + s_n) &= \exp\left[-\int_D^{x_0} a l^{a-1} (t - t_n + s_n) \exp(\beta_1 z_{2,1})\,\mathrm{d}l\right] \\ &= \exp\left[-(x_0^a - D^a)(t - t_n + s_n) \exp(\beta_1 z_{2,1})\right] \end{aligned} \tag{14}$$

where

$$s_n = \frac{(t_n - t_{n-1} + s_{n-1}) \exp(\beta_n z_{1,n})}{\exp(\beta_1 z_{2,1})}. \tag{15}$$

Consequently, on the basis of equations (6) and (9), the reliability function for the ith profile in the jth cycle can be generalized as

$$R_{i,j} = \exp\left[-Q_{i,j} \cdot (\tau_i \cdot r_j + s_{(i-1)n+j-1}) \cdot \exp(\beta_j z_{i,j})\right] \tag{16}$$

where $Q_{i,j} = x_0^a - D^a$ when the stress affects only the degradation rate, $Q_{i,j} = x_0^a - (D + Kz_{i,j})^a$ when the stress simultaneously affects the degradation rate and degradation level, and

$$\begin{aligned} s_{(i-1)n+j-1} &= \sum_{g=1}^{i} \sum_{e=1}^{(g-1)n+j-1} \tau_g \cdot r_{e-(g-1)n} \\ &\quad \times \exp\left(\beta_{e-(g-1)n} z_{g,(e-(i-1)n)} - \beta_j z_{i,j}\right). \end{aligned} \tag{17}$$

3. Optimal design for CCSADT based on the D-optimality criterion

This section first describes the construction of the Fisher information matrix according to the likelihood function of the PHM parameters as per the aforementioned reliability function. Subsequently, the construction of the optimization model based on the D-optimality criterion is described to obtain the optimal CCS test scheme.

3.1. Optimization objective construction based on the D-optimality criterion

As the purpose of conducting the ADT is typically to improve the precision of the parameter estimators, the D-optimality design is applied herein to arrive at the CCSADT design. The D-optimality criterion is one of the most commonly employed in test design and parameter estimation, and its core objective is to enhance the stability and accuracy of parameter estimation in the ADM. According to Ma and Meeker [31], the asymptotic variance-covariance matrix of estimators of the ADM is always associated with the inverse of the Fisher information matrix, i.e.:

$$\mathrm{cov}\left(\hat{\delta}\right) = \frac{\sigma^2}{N} F^{-1} \tag{18}$$

where F represents the Fisher information matrix, $\hat{\delta}$ represents the estimator vector of unknown parameters in the accelerated degradation model, σ^2 represents the variance of the random error, and N represents the number of samples.

Therefore, the D-optimality criterion is applied to minimize the determinant of the covariance matrix of $\hat{\delta}$, or, equivalently, to maximize the determinant of the Fisher information matrix, thereby guaranteeing that the precision of parameter estimation is maximized. The definition of an information matrix is the expectation of the second derivative of a negative log-likelihood function with respect to the parameters, as shown in equation (19). Thus, the first step is to obtain the likelihood function.

$$F = E\left[-\frac{\partial^2 \ln L}{\partial \delta \partial \delta^T}\right]. \tag{19}$$

If the degradation level of N samples measured during the test is $\{X_{i,j,c}; i=1,2,\cdots,m, j=1,2,\cdots,n, c=1,2,\cdots,N\}$, the probability of the measurement $X_{i,j,c}$ according to equations (6) and (16) can be calculated as:

$$\begin{aligned} f(X_{i,j,c};t,z) &= h(X_{i,j,c};t,z)R(t) \\ &= aX_{i,j,c}^{a-1}t\exp(\beta_j z_{i,j})\exp\left[-Q_{i,j}\cdot\exp(\beta_j z_{i,j})\right. \\ &\quad\times\left(\tau_i\cdot r_j+\sum_{g=1}^{i}\sum_{e=1}^{(g-1)n+j-1}\tau_g\cdot r_{e-(g-1)n}\right. \\ &\quad\left.\left.\times\exp(\beta_{e-(g-1)n}z_{g,(e-(i-1)n)}-\beta_j z_{i,j})\right)\right]. \end{aligned} \tag{20}$$

Therefore, by integrating the probabilities of all the degradation measurements, the log-likelihood function of the PHM parameters can be obtained as:

$$\begin{aligned} \ln L = \sum_{i=1}^{m}\sum_{j=1}^{n}\sum_{c=1}^{N}\Bigg[&\ln a+(a-1)\ln X_{i,j,c}+\ln t+\beta_j z_{i,j} \\ &-Q_{i,j}\cdot\exp(\beta_j z_{i,j})\cdot\left(\tau_i\cdot r_j+\sum_{g=1}^{i}\sum_{e=1}^{(g-1)n+j-1}\right. \\ &\left.\times\tau_g r_{e-(g-1)n}\exp\left(\beta_{e-(g-1)n}z_{g,(e-(g-1)n)}-\beta_j z_{i,j}\right)\right)\Bigg]. \end{aligned} \tag{21}$$

Finally, if the negative expectation for the second-order partial derivative of the log-likelihood function is considered with respect to the unknown parameters of the PHM, the Fisher information matrix can be obtained as:

$$F=\begin{bmatrix} E\left(-\frac{\partial^2\ln L}{\partial\beta_1^2}\right) & \cdots & E\left(-\frac{\partial^2\ln L}{\partial\beta_1\partial\beta_q}\right) & \cdots & E\left(-\frac{\partial^2\ln L}{\partial\beta_1\partial\beta_n}\right) & E\left(-\frac{\partial^2\ln L}{\partial\beta_1\partial a}\right) & E\left(-\frac{\partial^2\ln L}{\partial\beta_1\partial K}\right) \\ & \ddots & \vdots & \vdots & \vdots & \vdots & \vdots \\ & & E\left(-\frac{\partial^2\ln L}{\partial\beta_q^2}\right) & & E\left(-\frac{\partial^2\ln L}{\partial\beta_q\partial\beta_n}\right) & E\left(-\frac{\partial^2\ln L}{\partial\beta_q\partial a}\right) & E\left(-\frac{\partial^2\ln L}{\partial\beta_q\partial K}\right) \\ & & & \ddots & \vdots & \vdots & \vdots \\ & & & & E\left(-\frac{\partial^2\ln L}{\partial\beta_n^2}\right) & E\left(-\frac{\partial^2\ln L}{\partial\beta_n\partial a}\right) & E\left(-\frac{\partial^2\ln L}{\partial\beta_n\partial K}\right) \\ & \text{Symmetric} & & & & E\left(-\frac{\partial^2\ln L}{\partial a^2}\right) & E\left(-\frac{\partial^2\ln L}{\partial a\partial K}\right) \\ & & & & & & E\left(-\frac{\partial^2\ln L}{\partial K^2}\right) \end{bmatrix} \tag{22}$$

where

$$E\left(-\frac{\partial^2\ln L}{\partial\beta_j{}^2}\right)=\sum_{i=1}^{m}\sum_{j=1}^{n}\sum_{c=1}^{N}\left[\int_D^{x_0}(X_{i,j,c}-D)^a\lambda\mathrm{d}X_{i,j,c}\cdot\left[\left(z_{i,j}{}^2\tau_i\cdot r_j\cdot\exp(\beta_j z_{i,j})+\sum_{i=1}^{m-1}z_{i,j}{}^2\tau_i\cdot r_j\exp(\beta_j z_{i,j})\right)\right]\right]$$

$$E\left(-\frac{\partial^2\ln L}{\partial\beta_q{}^2}\right)=\sum_{i=1}^{m}\sum_{c=1}^{N}\left[\int_{D+Kz_{i,q}}^{x_0}(X_{i,q,c}-(D+Kz_{i,q}))^a\xi\,\mathrm{d}X_{i,q,c}\ \cdot\left(z_{i,q}{}^2\tau_i r_q\ \exp(\beta_q z_{i,q})+\sum_{i=1}^{m-1}z_{i,q}{}^2\tau_i\cdot r_q\exp(\beta_q z_{i,q})\right)\right]$$

$$E\left(-\frac{\partial^2\ln L}{\partial a^2}\right)=\sum_{i=1}^{m}\sum_{j=1}^{n}\sum_{c=1}^{N}\left[\frac{1}{a^2}+\theta_{i,j}\int_D^{x_0}(X_{i,j,c}-D)^a\ \cdot(\ln(X_{i,j,c}-D))^2\lambda\mathrm{d}X_{i,j,c}\right]$$

$$\begin{aligned} E\left(-\frac{\partial^2\ln L}{\partial K^2}\right)=\sum_{i=1}^{m}\sum_{c=1}^{N}\Bigg[&z_{i,q}{}^2(a-1)\int_{D+Kz_{i,q}}^{x_0}(X_{i,q,c}-(D+Kz_{i,q}))^{-2}\ \cdot\xi\,dX_{i,q,c}+z_{i,q}{}^2a(a-1)\theta_{i,q} \\ &\cdot\int_{D+Kz_{i,q}}^{x_0}(X_{i,q,c}-(D+Kz_{i,q}))^{a-2}\xi\,\mathrm{d}X_{i,q,c}\Bigg] \end{aligned}$$

$$E\left(-\frac{\partial^2\ln L}{\partial\beta_j\partial a}\right)=\sum_{i=1}^{m}\sum_{j=1}^{n}\sum_{c=1}^{N}\left[\int_D^{x_0}(X_{i,j,c}-D)^a\ln(X_{i,j,c}-D)\,\lambda\mathrm{d}X_{i,j,c}\ \left(z_{i,j}\tau_i\cdot r_j\exp(\beta_j z_{i,j})+\sum_{i=1}^{m-1}z_{i,j}\tau_i\cdot r_j\exp(\beta_j z_{i,j})\right)\right]$$

$$E\left(-\frac{\partial^2 \ln L}{\partial \beta_q \partial a}\right)=\sum_{i=1}^{m}\sum_{c=1}^{N}\left[\int_{D+Kz_{i,q}}^{x_0}\left(X_{i,q,c}-(D+Kz_{i,q})\right)^{a}\cdot\xi\ln\left(X_{i,q,c}-(D+Kz_{i,q})\right)\mathrm{d}X_{i,q,c}\left(z_{i,q}\tau_i\cdot r_q\right.\right.$$
$$\left.\left.\cdot\exp\left(\beta_q z_{i,q}\right)+\sum_{i=1}^{m-1}z_{i,q}\tau_i\cdot r_q\exp\left(\beta_q z_{i,q}\right)\right)\right]$$

$$E\left(-\frac{\partial^2 \ln L}{\partial \beta_q \partial K}\right)=\sum_{i=1}^{m}\sum_{c=1}^{N}\left[az_{i,q}\int_{D+Kz_{i,q}}^{x_0}\left(X_{i,q,c}-(D+Kz_{i,q})\right)^{a-1}\cdot\xi\,\mathrm{d}X_{i,q,c}\left(z_{i,q}\tau_i r_q\exp\left(\beta_q z_{i,q}\right)\right.\right.$$
$$\left.\left.+\sum_{i=1}^{m-1}z_{i,q}\tau_i r_j\exp\left(\beta_q z_{i,q}\right)\right]\right.$$

$$E\left(-\frac{\partial^2 \ln L}{\partial a \partial K}\right)=-\sum_{i=1}^{m}\sum_{c=1}^{N}z_{i,q}\theta_{i,q}\left[a\int_{D+Kz_{i,q}}^{x_0}\left(X_{i,q,c}-(D+Kz_{i,q})\right)^{a-1}\cdot\xi\ln\left(X_{i,q,c}-(D+Kz_{i,q})\right)\mathrm{d}X_{i,q,c}\right.$$
$$\left.+\int_{D+Kz_{i,q}}^{x_0}\left(X_{i,q,c}-(D+Kz_{i,q})\right)^{a-1}\xi\,dX_{i,q,c}\right]$$

and

$$\theta_{i,j}=\left[\tau_i\cdot r_j\exp\left(\beta_j z_{i,j}\right)+\sum_{g=1}^{i}\sum_{e=1}^{(g-1)n+j-1}\tau_g\cdot r_{e-(g-1)n}\right.$$
$$\left.\times\exp\left(\beta_{e-(g-1)n}z_{g,(e-(g-1)n)}\right)\right]$$

$$\theta_{i,q}=\left[\tau_i\cdot r_q\exp\left(\beta_q z_{i,q}\right)+\sum_{g=1}^{i}\sum_{e=1}^{(g-1)n+q-1}\tau_g\cdot r_{e-(g-1)n}\right.$$
$$\left.\times\exp\left(\beta_{e-(g-1)n}z_{g,(e-(g-1)n)}\right)\right]$$

$$\lambda=aX_{i,j,c}^{a-1}\theta_{i,j}\cdot\exp\left[-(X_{i,j,c}-D)^{a}\theta_{i,j}\right]$$

$$\xi=aX_{i,q,c}^{a-1}\theta_{i,q}\cdot\exp\left[-(X_{i,q,c}-(D+Kz_{i,q}))^{a}\theta_{i,q}\right].$$

Particularly, in equation (22), the contributions of each section to the logarithmic likelihood function are independent of one another.

3.2. Design variables

The optimality criterion of the CCSADT is to maximize the determinant of the Fisher information matrix, thereby maximizing the precision of the parameter estimators. According to assumption (3) and the expression in equation (22), the determinant value of the information matrix can be found as being related to the number of cycles m, stress magnitude of each profile $z_{i,j}$, and duration of each profile τ_i. Therefore, the design variables for the CCSADT plan are $\{m, z_{i,j}, \tau_i; i=1,2,\cdots,m, j=1,2,\cdots,n\}$.

3.3. Constraints establishment

In engineering practice, test resources primarily include test costs and test time. Therefore, this study constructs the constraints of the optimization model on the basis of these two resources.

(1) Constraint on test time
According to the description in section 2.1, as the time proportion of each profile within a single cycle is constant, the total test time is determined by the test duration of each cycle. Therefore, the constraint on the test time can be expressed as:

$$\sum_{i=1}^{m}\tau_i\leqslant\tau_{\mathrm{s}} \tag{23}$$

where τ_{s} is the maximum allowable test time.

(2) Constraint on test cost
In this study, three types of cost are considered, i.e. the sample cost of a single C_{s}, measurement cost C_i, and public resources consumed per unit time C_{p}. Therefore, the constraint on test cost can be expressed as

$$N\sum_{i=1}^{n\cdot m}C_i+NC_{\mathrm{s}}+\tau_{\mathrm{s}}C_{\mathrm{p}}\leqslant C_{\mathrm{t}} \tag{24}$$

where C_{t} is the maximum allowable test cost.

3.4. Construction and solution of CCSADT optimization design model

The objective of this study is to optimize the number of cycles in the CCSADT, stress levels under each profile, and duration of each profile while maximizing the determinant of the

information matrix. Therefore, from equations (23) and (24), the CCSADT optimization design model can be expressed as:

$$\text{Maximize } \det|F| \tag{25a}$$

$$\textit{Subject to: } z_l < z_{i,j} < z_h, i = 1,2,\cdots,m, j = 1,2,\cdots,n, \tag{25b}$$

$$\sum_{i=1}^{m} \tau_i \leqslant \tau_s, \tag{25c}$$

$$N\sum_{i=1}^{n\cdot m} C_i + NC_s + \tau_s C_p \leqslant C_t. \tag{25d}$$

In the aforementioned optimization model, equation (25*a*) indicates that the information matrix needs to be maximized, constraint (25*b*) indicates that the test level should be within the stress level range, and Constraints (25*c*) and (25*d*) indicate that the total test time and total test cost should not exceed their respective maximum allowable values.

For an optimization model such as in equation (25), several studies typically adopt genetic algorithms to obtain the solution. For example, Liu *et al* [32] adopted the genetic algorithm to solve the multi-objective ADT optimization design model, and Kong *et al* [33] adopted the genetic algorithm to solve the selective maintenance optimization model involving multiple components, multiple differences, and S-dependent influences. Therefore, this study also adopts genetic algorithms to solve the optimization problem.

4. Example analysis

This section provides a numerical example on electrical connectors to evaluate the effectiveness of the proposed method.

4.1. Example introduction

As described in section 1, the electrical connector is a key component in weapons and equipment. It successively traverses the storage profile, transportation profile, and test profile along with weapons and equipment; resultantly, its contact performance gradually degrades owing to oxidation on the surface of the contact parts. Particularly, in the storage, transportation, and test profiles, the electrical connector is primarily subjected to temperature stress T, vibration stress G, and electrical stress V, respectively. Among these, temperature and electrical stresses affect the degradation rate by accelerating oxidation reactions; concurrently, vibration not only accelerates wear and the breakdown of oxide films but also causes loosening of the contact structure, resulting in a sudden change in contact resistance. Therefore, a significant impact on both the degradation rate and the degradation state of contact performance is evident. According to Elsayed and Zhang [34], the Arrhenius model is commonly employed to capture the effect of temperature on the degradation performance of products, whereas the inverse power law model is adopted for capturing the effects of electrical stress and vibration, and their respective expressions are:

Table 1. Model parameters.

Parameters	β_1	β_2	β_3	a	K
Value	1.05	0.2098	0.857	3.37	0.25

$$\eta = A\exp\left(\frac{Ea}{kz}\right) \tag{26}$$

$$\eta = Bz^{-d} \tag{27}$$

where η represents the lifespan characteristic of the product, A and B are two constants, Ea and d are the activation energies, k is the Boltzmann constant, and z is the stress. Given that the characteristic lifetimes are all proportional to the reciprocal of the stress in equations (26) and (27), let z in equation (6) be expressed as $\frac{1}{T}$, $\frac{1}{G}$, and $\frac{1}{V}$ for the storage, transportation, and test profiles, respectively. In addition, as mentioned in the Introduction section, the vibration stress affects not only the degradation rate but also causes instantaneous damage on contact resistance, and the induced instantaneous damage is proportional to the stress level with a correlation coefficient K.

Before the optimization design is arrived at, the model parameters, which serve as the foundations for subsequent design and analyzes, should first be eliminated. In this study, the distance between the contact resistance and failure threshold is considered as the indicator of contact performance. To reflect the degradation performance due to the contact resistance under these profiles more accurately, this study estimates the parameters in the model on the basis of the test data of the electrical connector at the temperature value per [24] and the test data of the electrical connector at the vibration value per [35] while making reasonable assumptions for other model parameters. Thus, the parameter values of the PHM in equation (6) are obtained as listed in table 1.

One sample is tested, and the temperature stress level range is [298 K, 398 K], vibration stress level range is [0.2 g^2 Hz^{-1}, 0.8 g^2 Hz^{-1}], and electrical stress level range is [12 V, 18 V]. The initial distance between the initial contact resistance and failure threshold of the product is $x_0 = 30$ m Ω, and the failure threshold D is 0. Moreover, the cost of each sample is 500 RMB, monitoring cost for each time duration is 100 RMB, public resource consumption per unit time is 2 RMB, total test cost is constrained at 10 000 RMB, and total test time is constrained at 2000 h.

After the parameters are determined, the genetic algorithm is adopted to solve the optimization model in equation (25). Specifically, the GA function in MATLAB R2024b is used for the solution, where the initial population size is set to 200, the number of iterations is set to 500, and the parameters related to crossover probability, mutation probability, and stop threshold were all set to their default values. The results thereof are listed in table 2, from which the optimal number of test cycles under the constraints of the given test time and cost can be deduced to be 6; among these cycles, the levels of each stress alternate up and down rather

Table 2. Optimization design of CCSADT with electrical connector.

Test profiles	$T(K)$	$G\left(\mathrm{g}^2\,\mathrm{Hz}^{-1}\right)$	$V(V)$	during time (h)
1	298.22	0.7964	12.25	194.02
2	298.53	0.2008	12.16	252.65
3	301.33	0.5559	12.69	6.30
4	306.01	0.7500	16.48	145.38
5	309.59	0.7498	12.93	65.31
6	308.10	0.2008	12.77	135.25

Table 3. Test scheme by UD.

Test profiles	$T(K)$	$G\left(\mathrm{g}^2\,\mathrm{Hz}^{-1}\right)$	$V(V)$	during time (h)
1	298.15	0.20	12.0	333.33
2	318.15	0.56	14.4	333.33
3	338.15	0.32	13.2	333.33
4	358.15	0.68	15.6	333.33
5	378.15	0.44	16.8	333.33
6	398.15	0.80	18.0	333.33

than decreasing or increasing monotonically. Moreover, an increase in the levels of temperature, vibration stress, and electrical stress leads to a reduction in cycle duration; conversely, a decrease in these factors results in a longer cycle duration.

4.2. Comparative analysis

To verify the validity of the proposed method, the method is compared with the commonly adopted uniform design (UD), Latin hypercube sampling design (LHSD), and the CSADT under the same test cost and test time constraints.

Specifically, to construct the UD, from the results of the 6 optimized stress levels obtained in table 2, 6 stress levels are respectively considered for the temperature range of 298–398 K, vibration range of 0.2–0.8 $\mathrm{g}^2\,\mathrm{Hz}^{-1}$, and electrical stress range of 12–18 V. Correspondingly, the UD table $U(6,3)$ is employed to design the test, and the result thereof is summarized in table 3. For the LHSD, the range of all stress levels is identical to that specified in UD. In the LHSD, each stress range is uniformly partitioned into 6 non-overlapping sub-intervals, and one stress level is randomly selected from each sub-interval. Subsequently, the selected levels across all stresses are randomly permuted and combined to generate the final design presented in table 4. Finally, for the CSADT, a single cycle of CS with the mean values of each stress level listed in table 2 as the applied stress levels is performed and presented in table 5. Additionally, the determinant value of the Fisher information matrix of these two test schemes is calculated; according to [36], the relative efficiency (RE) is applied to quantify the improvement in relative estimation accuracy of the parameters under the proposed method, which is defined as:

Table 4. Test scheme by LHSD.

Test profiles	$T(K)$	$G\left(\mathrm{g}^2\,\mathrm{Hz}^{-1}\right)$	$V(V)$	during time (h)
1	305.21	0.69	18.0	200
2	388.57	0.36	13.6	250
3	321.89	0.80	15.8	310
4	355.23	0.25	12.5	340
5	338.56	0.58	16.9	380
6	371.90	0.47	14.7	520

Table 5. Test scheme by CSADT.

Test profiles	$T(K)$	$G\left(\mathrm{g}^2\,\mathrm{Hz}^{-1}\right)$	$V(V)$	during time (h)
1	303.63	0.5424	13.2	2000

Table 6. Comparison of the test scheme under four methods.

Method	$\det F$	RE
Proposed method	3.1717×10^{18}	100%
UD	1.0440×10^{18}	203.8%
LHSD	9.138×10^{17}	247.09%
CSADT	4.4×10^{17}	620.8%

$$RE = \frac{\det F_P \text{ - } \det F_{CD}}{\det F_{CD}} \times 100\% \tag{28}$$

where $\det F_{\mathrm{P}}$ and $\det F_{\mathrm{CD}}$ represent the determinant values of the Fisher information matrix of the test scheme obtained via the proposed method and the contrast design, respectively.

The comparison results are listed in table 6, from which the following conclusions can be drawn:

(1) The proposed CCSADT fully considers the cyclic alternating effects and cumulative damage characteristics of various stresses under real task profiles, which is consistent with the actual degradation process of products such as electrical connectors. In contrast, the UD and LHSD only focus on the spatial allocation of stress levels, whereas traditional CSADT applies stresses sequentially within a single cycle. All of these methods neglect the alternating cyclic effects of multiple stresses, resulting in significant deviations from actual operating conditions.
(2) The proposed method achieves the highest parameter estimation accuracy under the same test time and cost constraints. The determinant of the Fisher information matrix obtained by the proposed method is 3.04 times, 3.47 times, and 7.21 times that of UD, LHSD, and CSADT, respectively. Correspondingly, the RE is decreased by 103.8%, 147.09%, and 520.8%, respectively, indicating that the proposed CCSADT can provide more effective information for model parameter estimation.
(3) The proposed method is more flexible and practical in engineering applications. It can simultaneously optimize the number of cycles, stress levels, and test duration of each stage under given test time and cost limits, thereby maximizing the test efficiency.

These results fully prove that the proposed CCSADT is more suitable for the reliability assessment of products with multi-task cyclic characteristics and stage-sensitive stresses.

4.3. Sensitivity analysis of parameters

The performance of the proposed optimal test scheme depends on the pre-specified model parameters β_1, β_2, β_3, a, and K. However, these parameters are typically unknown *a priori*, and their initial values must be estimated using prior information. Such estimates inevitably deviate from the true parameter values to some extent. Therefore, to rigorously assess the robustness of the proposed method and to provide a basis for parameter accuracy requirements, a systematic sensitivity analysis of model parameters to the optimal test scheme formulation is essential. Similar to [37], the relationship between the pre-estimators and the true parameters is expressed as:

$$\left[\hat{\beta}_1, \hat{\beta}_2, \hat{\beta}_3, \hat{a}, \hat{K}\right] = \left[(1+\varepsilon_1)\beta_1, (1+\varepsilon_2)\beta_2, (1+\varepsilon_3) \times \beta_3, (1+\varepsilon_4)a, (1+\varepsilon_5)K\right] \tag{29}$$

where $\varepsilon_1 \sim \varepsilon_5$ denote the relative errors. Let $\det F_{\text{error}}$ denote the optimal determinant value derived from the estimated model parameters with various error combinations, and let $\det F_{\text{actual}}$ denote the determinant value of the test scheme obtained using the actual parameters listed in table 1, then the determinant efficiency (DE) introduced in [37] is used to measure the robustness of the proposed method, which is expressed as

$$\text{DE} = \frac{\det F_{\text{error}}}{\det F_{\text{actual}}} \times 100\%. \tag{30}$$

When conducting the sensitivity analysis, for each scenario, we introduce an estimation error in a single parameter while holding all other parameters at their actual values. The optimal test scheme under each scenario with the estimation error of 5% and 10% are presented in figures 3(a) and (b), respectively. Meanwhile, the corresponding DE for each scenario is reported in tables 7 and 8, respectively. From figures 3(a) and (b), it can be observed that within the estimation error of 5% and 10%, the overall variation range of the stress distribution scheme is relatively small. Besides, tables 7 and 8 reveal that when the estimation error is 5%, the DE of the optimal experimental design consistently exceeds 95% across all scenarios, and when the estimation error increases to 10%, the DE remains above 90%. This indicates that even in the presence of certain parameter estimation errors, the proposed method can still obtain test schemes that closely approximate the optimal test schemes derived under the actual parameters. Consequently, the robustness of the proposed method is verified.

4.4. Analysis of the impact of test time and cost

In practical engineering applications of the ADT, the total test time and test cost are typically the two most critical and restrictive types of test resources. The total test time directly determines the completeness of the degradation information that can be obtained and the feasible range of the test profile; concurrently, the cost of the test limits the number of tests, the configuration of stress levels, and the complexity of the test plan. Therefore, systematically analyzing the influence of the total test time and test cost constraints on the optimal test design results is necessary, which can provide a reference for

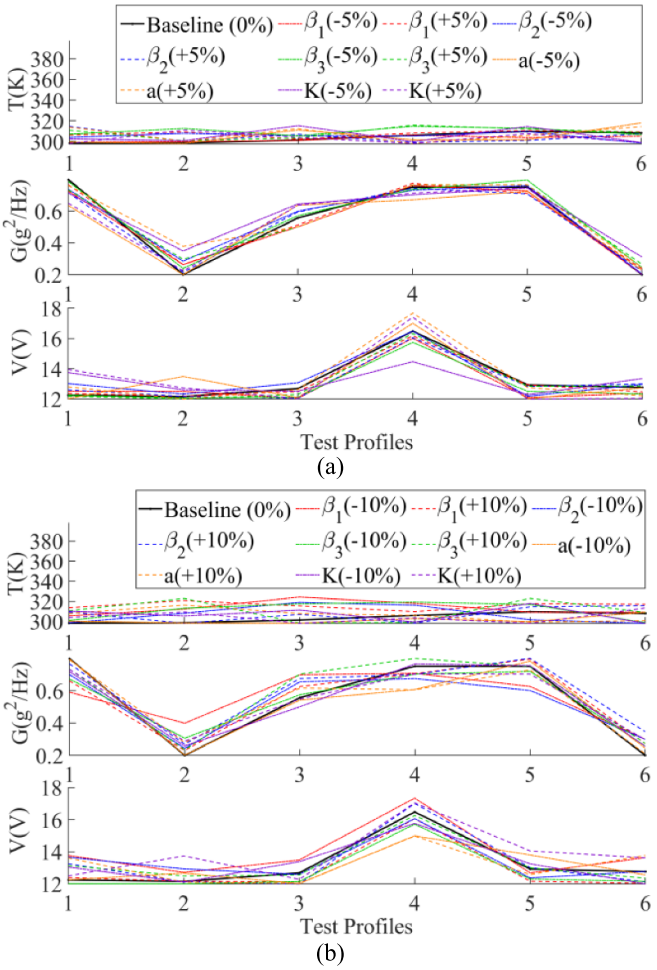


Figure 3. The test scheme under each scenario with the estimation error of (a) 5%, (b) 10%.

Table 7. The DE under various error combinations when the estimated error is 5%.

ε_1	ε_2	ε_3	ε_4	ε_5	DE
0%	0%	0%	0%	0%	100%
−5%	0%	0%	0%	0%	97.13%
+5%	0%	0%	0%	0%	96.35%
0%	−5%	0%	0%	0%	95.57%
0%	+5%	0%	0%	0%	98.17%
0%	0%	−5%	0%	0%	98.88%
0%	0%	+5%	0%	0%	99.36%
0%	0%	0%	−5%	0%	96.46%
0%	0%	0%	+5%	0%	95.56%
0%	0%	0%	0%	−5%	97.79%
0%	0%	0%	0%	+5%	96.83%

Table 8. The DE under various error combinations when the estimated error is 10%.

ε_1	ε_2	ε_3	ε_4	ε_5	DE
0%	0%	0%	0%	0%	100%
−10%	0%	0%	0%	0%	95.98%
+10%	0%	0%	0%	0%	93.39%
0%	−10%	0%	0%	0%	90.23%
0%	+10%	0%	0%	0%	93.34%
0%	0%	−10%	0%	0%	94.72%
0%	0%	+10%	0%	0%	92.01%
0%	0%	0%	−10%	0%	92.61%
0%	0%	0%	+10%	0%	90.25%
0%	0%	0%	0%	−10%	91.37%
0%	0%	0%	0%	+10%	90.29%

engineers to reasonably balance the accuracy of test information acquisition and consumption of test resources under actual conditions.

The CCSADT schemes under the conditions of test cost constraints of 10 000 RMB, 13 500 RMB, 17 000 RMB, 20 500 RMB, and 24 000 RMB, as well as test time constraints of 2000 h, 3000 h, 4000 h, 5000 h, and 6000 h, are considered, respectively, whereas other configurations remain unchanged. Particularly, for each case, the determinant values of the Fisher information matrix of the test scheme obtained via the proposed method and that obtained using the UD, LHSD, and CSADT are provided, and the RE is also calculated for comparison. The results are shown in figure 4. From figure 4(a), the increase in the test time and cost constraints results in an increase in the determinant values of the Fisher information matrix under all four methods, which indicates that under the condition of more abundant test resources, the test scheme can provide more effective information. Besides, it is seen that the proposed method always achieves the largest determinant value, which further highlights the effectiveness of the proposed method in developing efficient test schemes under constrained test resources. Conversely, figure 4(b) reveals that the RE values of the three compared methods relative to the proposed method consistently decrease as test resources increase. For the UD and LHSD, this trend occurs because longer test times and higher costs facilitate a greater number of cycles, which in turn increases the number of stress level combinations in the design. In contrast, for the CSADT design, the same trend stems from the fact that increased test time and cost yield more abundant degradation measurements. As a result, the test scheme derived from these three designs can also achieve progressively higher accuracy in parameter estimation. Furthermore, figure 4(a) shows that when the test time and cost constraints increase to a certain extent, the increased amplitude of the determinant value of the Fisher information matrix under the four methods gradually decreases, indicating that even if more test resources are added at this time, bringing about a significant improvement in experimental efficiency is difficult.

Consequently, based on figure 4, engineers can better understand the impact of test cost and time constraints on the formulation of the test scheme and the accuracy of parameter

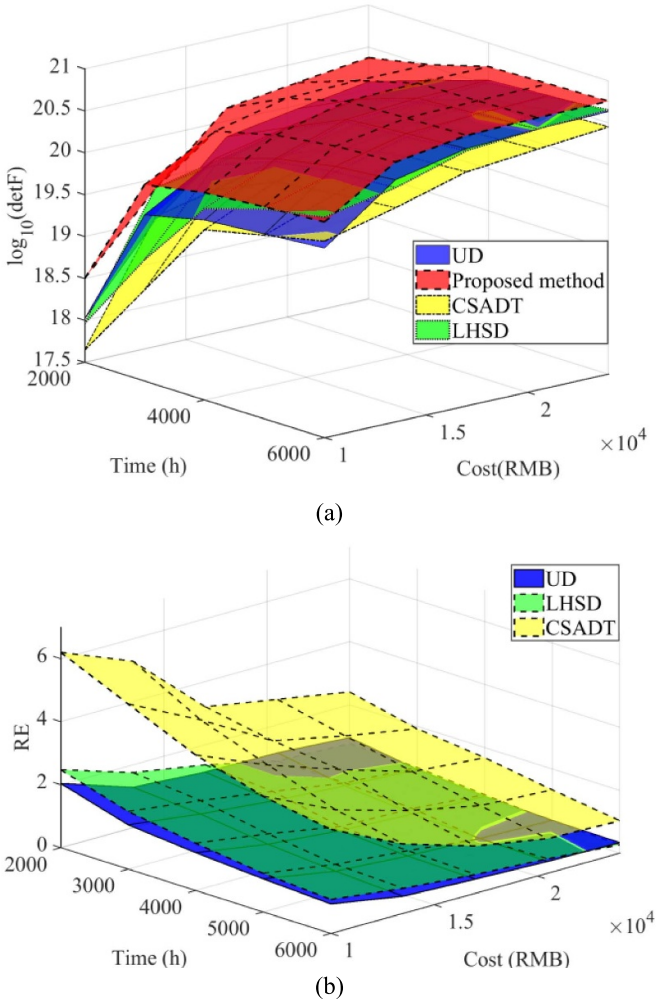


Figure 4. Comparison of the test schemes under two methods with different test times and costs: (a) det F, (b) RE.

estimation under this test scheme and thus select the appropriate cost and time constraints according to the actual assessment accuracy requirements.

5. Conclusion

To address the issue of frequently cycling through multiple different stages in actual task environments, this study adopts the PHM model that does not require assumptions about the degradation path. On this basis, combined with the cumulative damage theory, a reliability function under CCS is constructed. Subsequently, based on the D-optimality criterion, with the number of cycles, stress level, and the time required for each cycle as decision variables, the optimal test scheme was obtained. A comparison of the test scheme of the proposed method with those of UD, LHSD, and CSADT reveals that its RE decreases by 103.8%, 147.09%, and 520.8%, respectively, which benefits from the full consideration of the alternating cyclic effect of multiple stresses and cumulative damage mechanisms that are consistent with actual engineering scenarios. Therefore, it is proved that for products that need to

repeatedly undergo various mission profiles and have different sensitive stresses in each profile, the proposed method can provide the optimal solution for the number of required ADT, the duration time in each cycle, and the optimal stress levels according to the test cost and time constraint, thereby improving the test efficiency. Furthermore, a sensitivity analysis of the model parameters is conducted to assess the robustness of the proposed method. The results indicate that even with a $\pm 10\%$ estimation error in the parameters, the test scheme derived from the estimated parameters remains highly consistent with that obtained under the true parameter values, and the DE is maintained at a high level, thereby offering practical guidance for requirements on data measurement accuracy. Finally, the influence of the test cost and time constraint on the test results was also analyzed, based on which engineers can determine appropriate test resources according to the required parameter estimation accuracy requirements.

This study mainly focuses on the case where only one dominant sensitive stress exists in each working condition. However, in practical engineering applications, a single working condition is often simultaneously subjected to the coupling effect of multiple stresses. Therefore, in the future, the situation where a single profile is subjected to multiple stresses can be studied. Additionally, this study considers electronic products with a single performance index as the research object, whereas actual products usually have multiple key performance characteristics. Therefore, future research can be further expanded to multi-performance scenarios. Moreover, for the optimization model proposed in this paper, more efficient and stable solution algorithms can also be explored to enhance computational efficiency and engineering applicability.

Acknowledgments

This work is supported by the National Natural Science Foundation of China under Grant No. 72401261, the Funds of the Natural Science Foundation of Hangzhou under Grant No. 2025SZRJJ0777, and Zhejiang Provincial Leading Project for Leading Geese Plan under Grant No. 2024C01043.

ORCID iD

Xuefeng Kong 0000-0002-0490-7190

References

[1] Yu L, Hao X Tong K Hou W, Tian H and Han J 2024 *Appl. Comput. Eng.* **61** 129–36
[2] Li S, Yan Z and Jia J 2025 *Entropy* **27** 1197
[3] Wang Y, Wang G, Wu Y, Zhang G and Zheng R 2025 *Eksploat. Niezawodn.* **27** 203543
[4] Tang J and Zhou H 2025 *Sci. Rep.* **15** 31274
[5] Shat H and Schwabe R 2024 *Commun. Stat. Theory Methods* **53** 2154–77
[6] Zheng H Yang J Kang W and Zhao Y 2024 *Appl. Math. Modell.* **126** 420–38
[7] Kang M Lee S Kim J H Yoo C S Jang J Negatu B M and Park S 2022 *J. Mech. Sci. Technol.* **36** 4905–12
[8] Choi Y Kim M Park J and Goo Y 2025 *Appl. Sci. Basel* **15** 1300
[9] Yang L, Gao H, Chen H, Liu C, Yang Z and Zio E 2024 *Reliab. Eng. Syst. Saf.* **247** 110101
[10] Hu J and Chen P 2020 *Reliab. Eng. Syst. Saf.* **196** 106707
[11] Gao J Chen S Wang D Wang H and Zhao S 2026 *IEEE Trans. Power Electron.* **41** 5670–83
[12] Huang Q, Tang J and Feng X 2025 *PLoS One* **20** e0325117
[13] Jiang P Han J and Ma H 2022 *Equip. Environ. Eng.* **19** 13–20
[14] Li C, Cheng J, Zhu H, Wen B, Zhao X and Kang W 2025 *Sci. Rep.* **15** 19117
[15] Liu G Wang L Zhao X Yang Y and Liu D 2025 *J. Electr. Eng. Technol.* **20** 4551–8
[16] Zheng H, Kong X, Xu H and Yang J 2021 *Reliab. Eng. Syst. Saf.* **216** 107964
[17] Shrahili M, Kayid M and Mesfioui M 2023 *Mathematics* **11** 4652
[18] Yan W, Xu X, Bigaud D and Cao W 2023 *Reliab. Eng. Syst. Saf.* **230** 108917
[19] Wu W, Xu X and Liu W 2025 *Comput. Integr. Manuf. Syst.* **31** 3846–59
[20] Zhi L 2022 Univ. Electron. Sci. Technol. China 2023 1 (MA thesis) (https://doi.org/10.27005/d.cnki.gdzku.2022.004245)
[21] Li N, Gu D, Wang Z, Li S, Chen B and Chen P 2025 *Proc. Inst. Mech. Eng. O* **239** 496–514
[22] Jin A Yang Z Guo J Chen C and Liu Z 2026 *Qual. Technol. Quant. Manage.* **23** 1–17
[23] Ren L, Zhang X and Lan X 2025 *Appl. Sci.* **15** 3328
[24] Song Y 2020 Z. Sci. Tech. Univ. 2021 4 (MA thesis) (https://doi.org/10.27786/d.cnki.gzjlg.2020.000673)
[25] Li X 2024 Southwest Univ. Sci. Technol. 2025 5 (MA thesis) (https://doi.org/10.27415/d.cnki.gxngc.2024.001077)
[26] Xia H 2019 Z. Sci.Tech. Univ. 2019 6 (MA thesis) (available at: https://kns.cnki.net/kcms2/article/abstract?v=ZMT4ddBD2nwfyZ0O6IEz6LuUgC1s8onDrAuwb6sqHafqSY5cIrWhXAIGhnSsEvMQOcQVi6tfzMnXtiHlcRT-eE99qKL4nhOzsJSrm357SALTuCLybGdDOkRg2gVcqngZUv9fUG4VtB1S4Bf1m2obwVLXVF3BLeBV8Pn72iTKh0lDe8_OQVhjRFtvpDLW8DhS&uniplatform=NZKPT&language=CHS)
[27] Dong Y, Zhou Z, Liu K and Yang X 2024 *Appl. Sci.* **14** 8767
[28] Cai Z Chen Y and Li C 2018 *Electron. Opt. Control* **25** 64–67
[29] Eghbali G and Elsayed E A 2001 Dep. Ind. Eng. Rutgers Univ. (Ph.D. Thesis.) (available at: https://www.researchgate.net/publication/255665976_Reliability_Estimate_using_Degradation_Data)
[30] Wang P and Coit D W 2012 *2012 Int. Conf. on Quality, Reliability, Risk, Maintenance, and Safety Engineering (Icqr2mse)* pp 789–93
[31] Ma H and Meeker W Q 2008 *Nav. Res. Logist.* **55** 551–62
[32] Liu X Guo B Xia L, Tian X and Zhang L 2022 *Commun. Stat. Theory Methods* **51** 1426–43
[33] Kong X, Li L Chen W, Pan J and Yang J 2024 *Appl. Math. Modell.* **132** 561–86
[34] Elsayed E A and Zhang H 2007 *Reliab. Eng. Syst. Saf.* **92** 286–92
[35] Zhang W 2020 Zhejiang Sci-Tech University 2021 4 (MA thesis) (https://doi.org/10.27786/d.cnki.gzjlg.2020.000677)
[36] Hu C H Lee M Y and Tang J 2015 *Eur. J. Oper. Res.* **241** 412–21
[37] Zhang X Yang J and Kong X 2020 *Qual. Reliab. Eng. Int.* **37** 60–77



Xuefeng Kong is currently an Associate Professor with the School of Mechanical Engineering, Zhejiang Sci-Tech University, Zhejiang, China. His scientific interests include reliability modeling, accelerated test design, and maintenance optimization.



Yinjing Wang is currently pursuing a BS degree in mechanical engineering with the School of Mechanical Engineering, Zhejiang Sci-Tech University, Zhejiang, China. Her scientific interests include reliability modeling and accelerated test design.



Jun Pan is currently a Professor with the School of Mechanical Engineering, Zhejiang Sci-Tech University, Zhejiang, China. His research interests include failure physical analysis, reliability modeling, and accelerated life testing of mechanical and electrical products.



Wenhua Chen is currently a Professor with the School of Mechanical Engineering, Zhejiang Sci-Tech University, Zhejiang, China. His research interests include reliability analysis, design, and testing of mechanical and electrical products.